Optogenetic control of gene expression in plants in the presence of ambient white light

Rocio Ochoa-Fernandez [1,2], Nikolaj B. Abel [3], Franz-Georg Wieland [4], Jenia Schlegel[2,5], Leonie-Alexa Koch[1], J. Benjamin Miller [6], Raphael Engesser[4], Giovanni Giuriani[1,7], Simon M. Brandl[3], Jens Timmer[4,8], Wilfried Weber [3,8], Thomas Ott [3,8], Rüdiger Simon [2,5,9] and Matias D. Zurbriggen [1,2,9] ✉

Optogenetics is the genetic approach for controlling cellular processes with light. It provides spatiotemporal, quantitative and reversible control over biological signaling and metabolic processes, overcoming limitations of chemically inducible systems. However, optogenetics lags in plant research because ambient light required for growth leads to undesired system activation. We solved this issue by developing plant usable light-switch elements (PULSE), an optogenetic tool for reversibly controlling gene expression in plants under ambient light. PULSE combines a blue-light-regulated repressor with a red-light-inducible switch. Gene expression is only activated under red light and remains inactive under white light or in darkness. Supported by a quantitative mathematical model, we characterized PULSE in protoplasts and achieved high induction rates, and we combined it with CRISPR–Cas9-based technologies to target synthetic signaling and developmental pathways. We applied PULSE to control immune responses in plant leaves and generated *Arabidopsis* transgenic plants. PULSE opens broad experimental avenues in plant research and biotechnology.

The reversible and orthogonal control of cellular processes with high spatiotemporal resolution is key for quantitatively understanding the dynamics of biological signaling networks as well as for programming desired phenotypes. The optimal stimulus for such cellular control is light, as it can be applied with spatiotemporal precision in a quantitative manner with minimal toxicity and invasiveness. Accordingly, optogenetics, using genetically encoded, light-responsive switches, is widely utilized in mammalian systems, for example in processes such as neuromodulation, gene expression, epigenetics, protein and organellar activity and subcellular localization[1–7].

Although similar approaches are needed in plant research, the use of optogenetics is limited by plants' intrinsic need for broad-spectrum light, which would erroneously activate light-responsive switches. We have recently developed two optogenetic systems for the control of gene expression in plant cells. The systems are regulated by red and green light, and we have used them for the quantitative manipulation of hormone signaling pathways and control of recombinant-protein expression[8,9]. However, owing to spectral compatibility limitations and the need for cofactors that are difficult to administer to whole plants, these tools could only be applied in transiently transformed plant cells, such as mesophyll protoplasts from *Nicotiana tabacum* or *Arabidopsis thaliana*, and the moss *Physcomitrella patens*, which can be kept in the dark prior to optogenetic experiments[8–10]. Despite the utility of these tools for transient signaling studies in cell culture, it is desirable to have an optogenetic tool that is functional in whole plants and is insensitive to broad-spectrum white light to harness the full potential of optogenetics in the plant kingdom.

Here, we develop an optogenetic system for the control of gene expression in plants that is inactive under white light and can be activated with monochromatic red light. The system, termed PULSE, comprises two engineered photoreceptors that exert combinatorial activity over the regulation of transcription initiation: one represses gene expression under blue light (B_{Off}) and is engineered from the EL222 photoreceptor[11], and the other activates gene expression with red light (R_{On}) and is based on a phytochrome B (PhyB)–PIF6 optoswitch[8,10] (Fig. 1).

We initially characterized PULSE in *A. thaliana* protoplasts. PULSE provides quantitative and spatiotemporal reversible control over gene expression, achieving high induction rates of expression (of up to approximately 400-fold) while being in the 'off' state under white light or in the dark. We developed a mathematical model to quantitatively characterize the dynamic behavior of the system and to guide experimental design. We combined PULSE with a plant transcription factor (TF) or a CRISPR–Cas9-derived gene activator and showed its functionality for the light-controlled activation of both *Arabidopsis* and orthogonal promoters. Furthermore, we applied PULSE to confer light-inducible immunity in planta using *Nicotiana benthamiana* leaves as a model system, and tested its functionality in whole *Arabidopsis* transgenic plants. These results demonstrate the wide applicability of PULSE, opening up perspectives for the targeted spatiotemporal and quantitative study and reversible control of plant signaling and genetic and metabolic networks, as well as the implementation of this tool for biotechnological approaches.

Results

Design, implementation, and test of the PULSE system in plant cells. PULSE is an integrated optogenetic molecular tool that consists of two components: a module that activates gene expression under red light (R_{On}) and a second that ensures effective
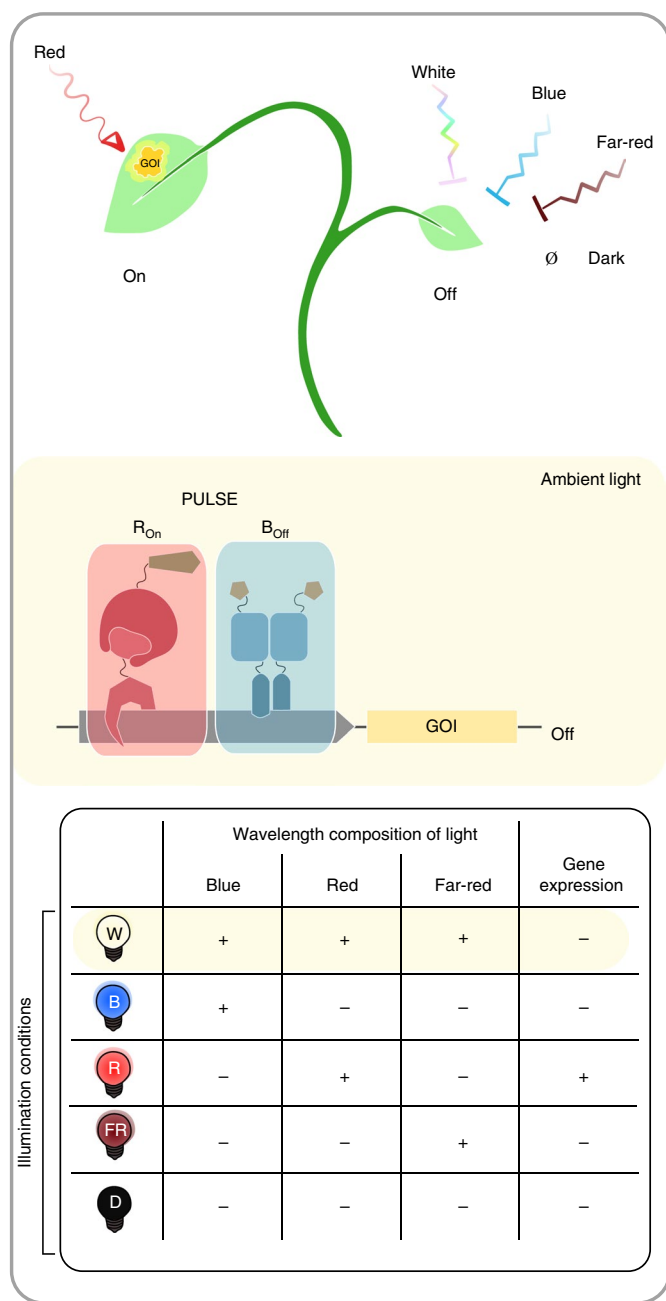
Fig. 1 | PULSE is an optogenetic system for the control of gene expression in plants grown under standard light–dark cycles. Schematic of PULSE (top). GOI, gene of interest; Ø, absence of light; B$_{Off}$, blue-light-regulated repressor; R$_{On}$, red-light-inducible gene-expression switch. Expected gene-expression outcome, depending on illumination conditions (bottom). W, white light; B, blue light; R, red light; FR, far-red light; D, darkness.

illumination, EL222 binds as a dimer to the target DNA sequence C120 (ref. [12]). B$_{Off}$ comprises the constitutively expressed EL222 fused to a transcriptional repressor domain (REP), and a reporter module driving the expression of a reporter gene (for example, firefly luciferase, *FLuc*) under the control of a synthetic tripartite promoter (Fig. 2a). The promoter comprises a quintuple-repeat target sequence for EL222, termed (C120)$_5$, flanked by the enhancer sequence of the CaMV35S promoter and the minimal domain of the constitutive promoter human cytomegalovirus (hCMV). In the dark, the EL222 photoreceptor is folded and unable to bind the (C120)$_5$ element; therefore, FLuc is constitutively expressed. Under blue light, EL222 binds the synthetic promoter, and thus switches the system off.

We evaluated three versions of the blue-light repressor module by fusing the amino terminus of EL222 to one of three trans-repressor domains: one from the protein containing human Krüppel-associated box (KRAB)[13,14], or one of two from *Arabidopsis*, namely the B3 repression domain (BRD)[15] and the EAR repression domain (SRDX)[15] (Fig. 2a). We assayed the functionality of the B$_{Off}$ optoswitches by transient cotransformation with the reporter construct into *Arabidopsis* protoplasts, and included constitutively expressed *Renilla* luciferase, RLuc, for normalization of data. We illuminated the cells for 18 h at different intensities of blue light (0, 0.25, 0.5, 1, 5 and 10 µmol m^{-2} s^{-1}) and quantified the FLuc/RLuc activity ratio (Fig. 2b). These blue-light intensities had no negative effect on protoplast performance. All 3 versions of the repressor modules were functional, although they had different efficiencies, yielding a range of repression levels (SRDX, 92%; BRD, 84%; and KRAB, 53%; at 10 µmol m^{-2} s^{-1} blue light). On the basis of it having the highest repression level and the dynamic range achieved, we used SRDX–EL222 as a trans-repressor module for all subsequent experiments.

To allow gene induction with PULSE, we combined the B$_{Off}$ module with our previously developed PhyB–PIF6 red-light-inducible split TF switch (R$_{On}$)[8,10] (Fig. 3a,b). PULSE thus integrates a constitutively expressed red-light activation module composed of PhyB–VP16 and E–PIF6; a constitutively expressed blue-light repressor module SRDX–EL222; and a synthetic target promoter, P$_{Opto}$. It integrates the binding domains for both switches, namely (C120)$_5$ and (etr)$_8$, upstream of a hCMV minimal promoter sequence driving the expression of a gene of interest. The rationale behind the mode of function of PULSE is that in the presence of monochromatic blue light or white light (a combination of blue, green, red and far-red wavelengths as present in ambient light), both photoreceptors PhyB and EL222 are predominantly in the active form, therefore binding to P$_{Opto}$. The net result of the recruitment of the transcriptional activator and repressor near the minimal promoter will set the system to the off state. The system will also be off in darkness and far-red-light conditions, as the red-light switch is rendered inactive under these conditions. Under any other illumination condition lacking the blue-light component, SRDX–EL222 is unable to bind P$_{Opto}$ and thus to repress transcription. The system is then in the 'on' state upon treatment with monochromatic red light, and the interaction between PhyB and PIF6 leads to the recruitment of the activation domain to the minimal promoter, inducing gene expression (Fig. 3a).

We tested the PULSE system in controlling FLuc expression in isolated *Arabidopsis* protoplasts (Fig. 3c). We transformed the plasmids encoding R$_{On}$ either with or without B$_{Off}$ and incubated the protoplasts for 18 h under red, blue, white or far-red light, or darkness. In the absence of the repressor module (equivalent to R$_{On}$), we observed efficient activation of PhyB by red, blue and white light, as ultraviolet and blue light (300–460 nm) also activate PhyB[16,17]. Upon addition of B$_{Off}$ (PULSE system), we observed induction under only red-light treatment, a high dynamic range of gene expression, with induction rates up to 396.5-fold above those in darkness, and

transcriptional repression under blue light (B$_{Off}$) (Fig. 1). The rationale behind this approach is that the combination of both switches will yield a system that is inactive in ambient growth conditions (light and darkness) and is only active upon irradiation with red light. This enables full applicability in plants growing under standard light conditions.

We first constructed a blue-light-regulated gene-repression switch, B$_{Off}$, based on the photoreceptor EL222 from the bacterium *Erythrobacter litoralis*[11], which has a light-oxygen-voltage (LOV) domain and a helix-turn-helix (HTH) domain. Upon blue-light
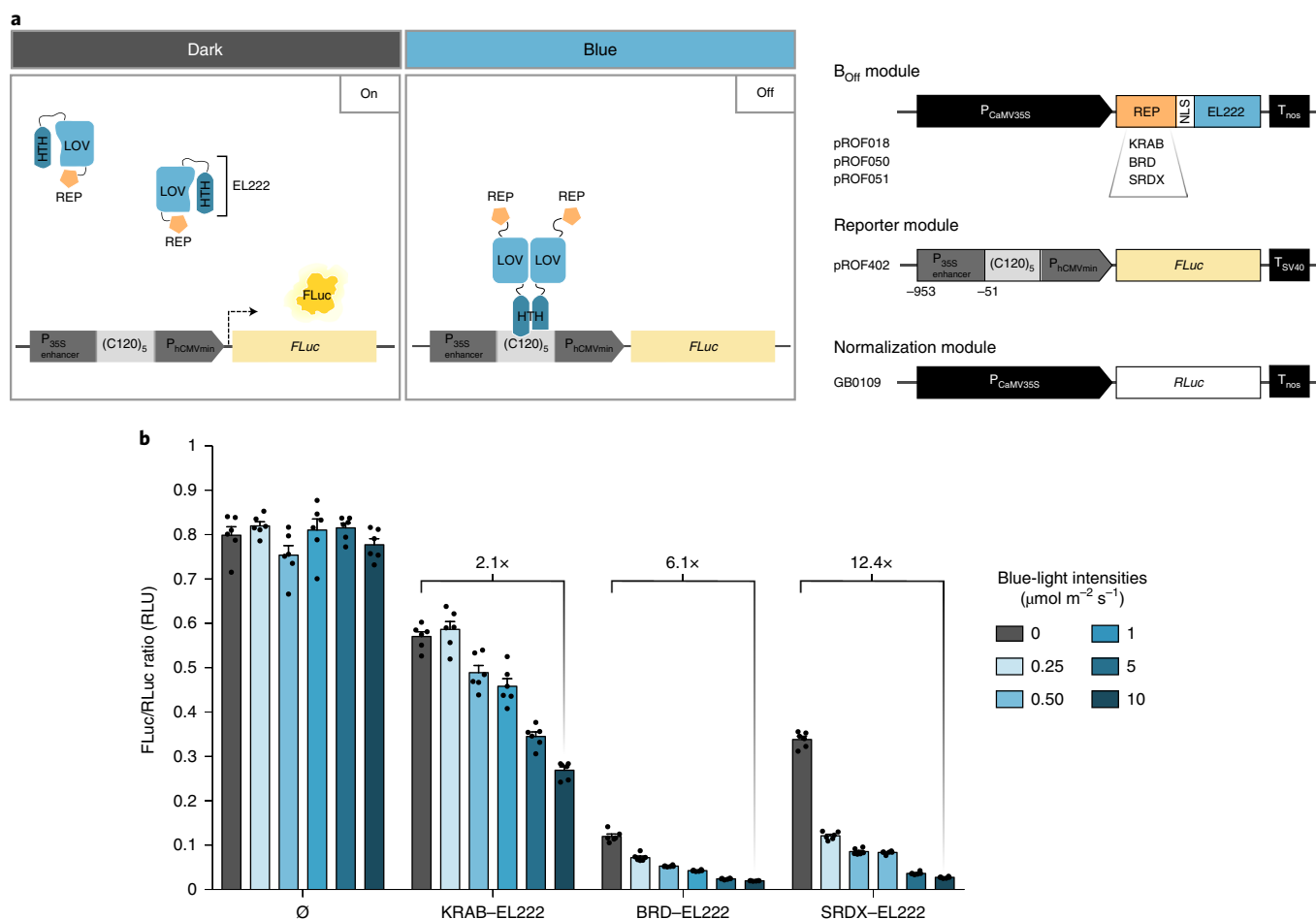
Fig. 2 | Characterization of B_Off in *Arabidopsis* protoplasts. a, Constructs and mode of function. The blue-light-responsive *E. litoralis* photoreceptor EL222 is fused to one of three different repressor domains (REP), KRAB, BRD or SRDX, and is placed under the control of the promoter P_CaMV35S. A synthetic promoter, composed of the enhancer region of P_CaMV35S, five repeats of the target DNA sequence of EL222, C120, and a minimal promoter P_hCMVmin, drives the expression of the reporter gene *FLuc*. P_CaMV35S drives the constitutive expression of *RLuc*. EL222 has a LOV domain and an HTH domain. **b**, FLuc activity in *Arabidopsis* protoplasts after transformation with the FLuc and RLuc modules and the indicated repressor modules or a control (∅). FLuc activity was normalized to RLuc activity. Protoplasts were kept in darkness or illuminated with the indicated intensities of blue light for 18 h. $n = 6$ protoplast samples for each condition; bars are the mean ratios, and error bars indicate s.e.m. RLU, relative luminescence units. NLS, nuclear localization sequence. T_nos, nopaline synthase terminator. T_SV40, SV40 virus terminator.

a low basal level of expression in blue and white light (1.7- and 1.6-fold, respectively).

Development and application of a quantitative model to describe and predict the PULSE activity. In order to quantitatively understand the dynamics and functional characteristics of PULSE and to guide the experimental design of future applications concerning optimal light quality, intensity and duration, we developed an ordinary differential equation (ODE)-based quantitative mathematical model (Supplementary Note). To parameterize the model, we performed on–off kinetic studies of the PULSE system in protoplasts by monitoring FLuc protein and messenger RNA levels (Extended Data Fig. 1a,b). The experiments demonstrate the reversibility of the system. In order to further characterize thresholds of time and light intensity for protein production, we collected end-point measurements and performed dose–response experiments (Supplementary Fig. 1). Next, we used the parameterized model to predict the experimental gene-expression outcomes of the system as a function of different light intensities, wavelengths and illumination times. We generated heatmaps based on simulations of the dynamic behavior of PULSE (Extended Data Fig. 1c and Supplementary Fig. 2), which

will aid in experimental design by guiding the targeted selection of conditions to obtain a given expression level of interest. To illustrate this, we tested combinations of red-light intensities and illumination durations selected from the heatmap. We observed a strong correspondence between predicted and experimentally determined activities (Extended Data Fig. 1c,d). This indicates the applicability of the model to determine the experimental conditions needed to achieve a tight control over the levels of gene expression with PULSE.

PULSE-controlled expression of CRISPR–Cas9-derived gene activator and plant TF. We next customized PULSE to achieve quantitative and temporally resolved control over the expression of genes from any given promoter of interest. We devised two approaches, inducing either the synthesis of a CRISPR–Cas9-derived gene activator or the expression of an endogenous TF. These transcriptional activators, in turn, activate expression from target orthogonal (Fig. 4a,b) or *Arabidopsis* promoters (Fig. 4c–f).

To achieve optogenetic and customizable control of potentially any target promoter, we used PULSE to control expression of a nuclease-deficient *Streptococcus pyogenes* Cas9 protein
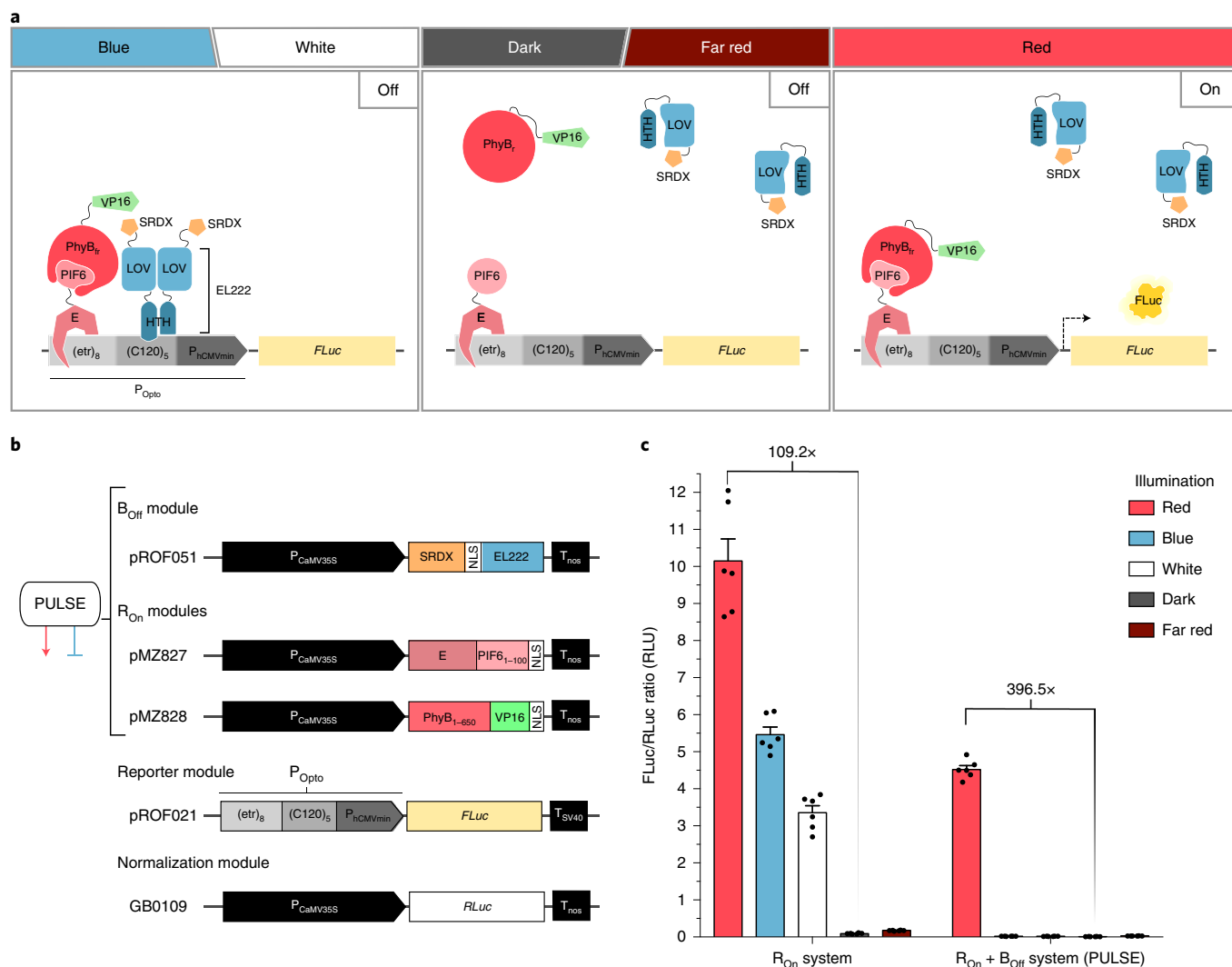
Fig. 3 | Characterization of PULSE in *Arabidopsis* protoplasts. a, Mode of function and state of the PULSE system under different illumination conditions. **b**, PULSE constructs. The SRDX-based B_{Off} module is combined with R_{On}, consisting of the first 650 amino acids of the PhyB photoreceptor ($PhyB_{1-650}$) fused to the VP16 transactivation domain, and the DNA-binding protein E 8mphR(A) fused to the first 100 amino acids of PIF6 (PIF_{1-100})[8]. The B_{Off} and R_{On} modules are constitutively expressed (promoter $P_{CaMV35S}$). A synthetic promoter P_{Opto}, comprising the target sequence of the protein E and of EL222, $(etr)_8$ and $(C120)_5$, and the minimal promoter $P_{hCMVmin}$ drives expression of FLuc. The RLuc construct is also included. **c**, Characterization of PULSE. FLuc/RLuc ratios of protoplast samples ($n = 6$ each) expressing either only the R_{On} module or the full PULSE system, in both cases including the reporter and normalization elements. FLuc and RLuc activities were determined 18 h after illumination. Protoplasts were kept in the dark or illuminated with white light, or 10 µmol m^{-2} s^{-1} of red ($\lambda_{max} = 655$ nm), blue ($\lambda_{max} = 461$ nm) or far-red ($\lambda_{max} = 740$ nm) light. Mean and s.e.m. are plotted. $PhyB_r$, red-light sensitive form of PhyB; $PhyB_{fr}$, far-red-light sensitive form of PhyB.

fused to a strong activation domain (termed dCas9–TV)[18,19]. In a first proof-of-principle application in *Arabidopsis* protoplasts, PULSE-induced dCas9–TV drove expression from an orthogonal promoter, the *Solanum lycopersicum* dihydroflavonol 4-reductase promoter (P_{SlDFR}), with FLuc as a quantitative readout (Fig. 4a). To target the promoter, we used a guide RNA against the –150-base-pair region relative to the transcription start site (TSS) of P_{SlDFR}[19]. PULSE-controlled dCas9–TV led to activation of the promoter only upon red-light illumination, achieving inductions of expression that were 24.5- and 40-fold over those in blue-light illumination and darkness, respectively (Fig. 4b). Constitutive expression of dCas9–TV served as a positive control, yielding the maximum activation capacity of P_{SlDFR} with 105.1-fold induction relative to the configuration without dCas9–TV (Supplementary Fig. 3a). In a second set of experiments, optogenetically induced dCas9–TV targeted the promoter of the *Arabidopsis* gene *AP1* (also known as floral homeotic protein APETALA1) (P_{AtAP1}), which includes the

5′ UTR and at 2,871 base pairs upstream of the TSS, cloned in a plasmid to drive expression of the reporter gene *FLuc* (P_{AtAP1}-FLuc). We designed a gRNA to target the –100-base-pair region relative to the TSS of P_{AtAP1} (Fig. 4c). Red-light induction of dCas9–TV yielded FLuc induction rates from the P_{AtAP1}–FLuc construct that were 17.9- and 14.1-fold over those in blue-light illumination and darkness, respectively (Fig. 4e). Constitutive expression of dCas9–TV yielded a 28.6-fold induction of expression relative to that in the configuration without dCas9–TV (Supplementary Fig. 3b).

We next configured PULSE to drive the expression of the *Arabidopsis* TF LEAFY (encoded by *LFY*), which binds P_{AtAP1} and promotes the expression of AP1 (ref. [20]). LFY and AP1 are involved in *Arabidopsis* flowering, and both are expressed in the floral primordia. We fused LFY to the transactivator VP16 and RLuc using a self-cleaving 2A sequence, which yields equimolar amounts of both proteins from a single transcript[21] (P_{Opto}–LFY–VP16–2A–RLuc). RLuc allows the indirect quantification of the synthesized amount
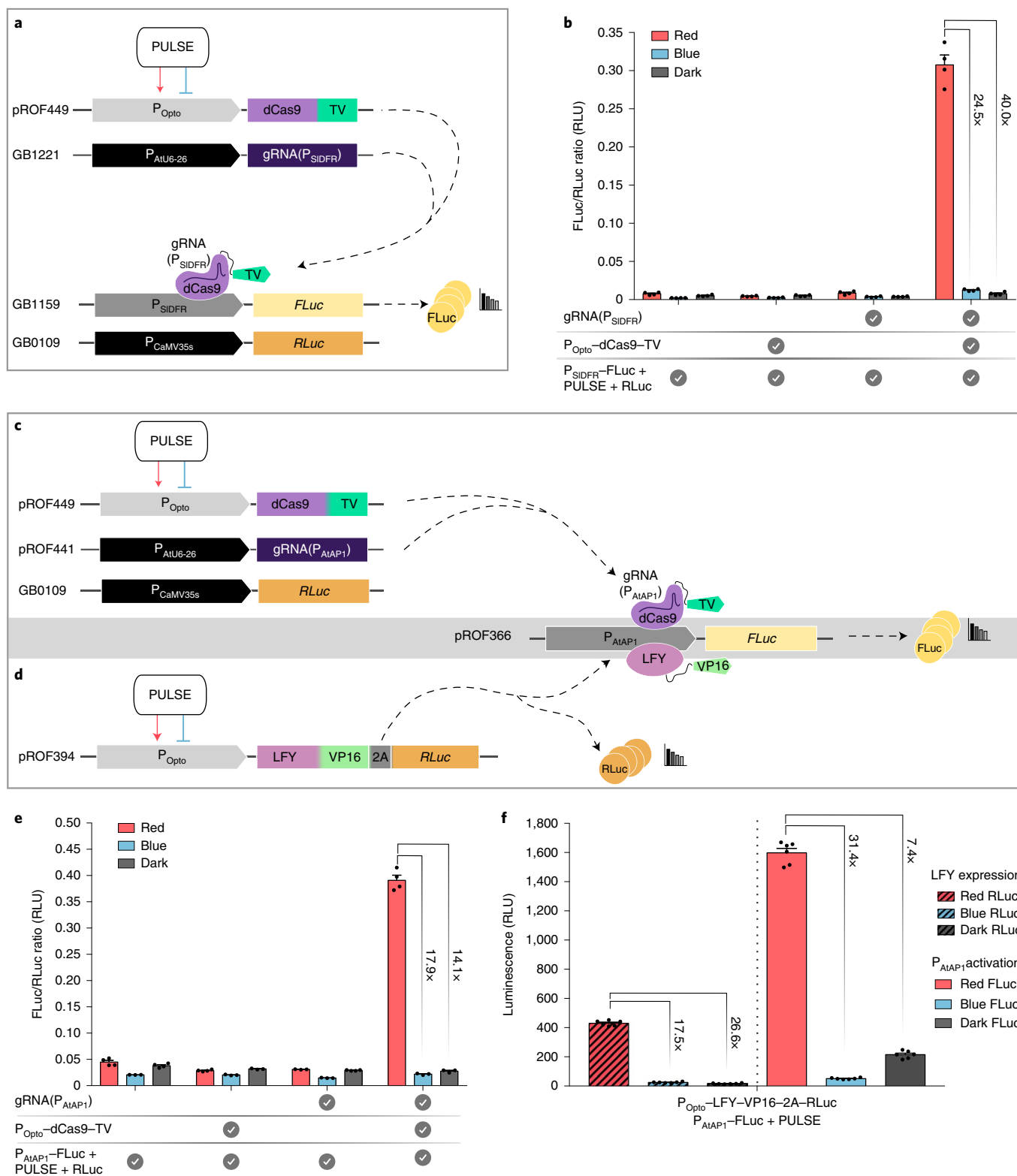
Fig. 4 | PULSE-controlled expression of a Cas9-derived gene activator (dCas9–TV) and an *Arabidopsis* transcription factor (LFY) in *Arabidopsis* protoplasts. a, Experimental outline for PULSE-driven dCas9–TV expression (P$_{Opto}$–dCas9–TV) under red light. dCas9–TV targets the orthogonal P$_{SlDFR}$ promoter. **b**, Normalized FLuc activity under the indicated experimental conditions. **c,d**, Experimental outline for PULSE-driven dCas9–TV and LFY–VP16 expression to control an *Arabidopsis* promoter, P$_{AtAP1}$, from a plasmid construct under red light. Coexpressed RLuc via a self-cleaving 2A peptide serves as proxy for LFY–VP16 expression. **e**, FLuc/RLuc ratios of protoplasts under the indicated experimental conditions. **f**, RLuc (proxy of LFY–VP16 expression, striped bars) and FLuc (P$_{AtAP1}$–FLuc activation, solid bars) in protoplasts under the indicated experimental conditions. In **b**, **e** and **f**, FLuc and RLuc activities were determined 18 h after illumination. Protoplasts were incubated in the dark, or illuminated with 10 µmol m^{-2} s^{-1} of red or blue light. Mean and s.e.m. are plotted for FLuc/RLuc ratios of $n=4$ protoplast samples (**b**,**e**) and luminescence of $n=6$ protoplast samples with background values (configuration without P$_{Opto}$–LFY–VP16–2A–RLuc) subtracted for FLuc (**f**).
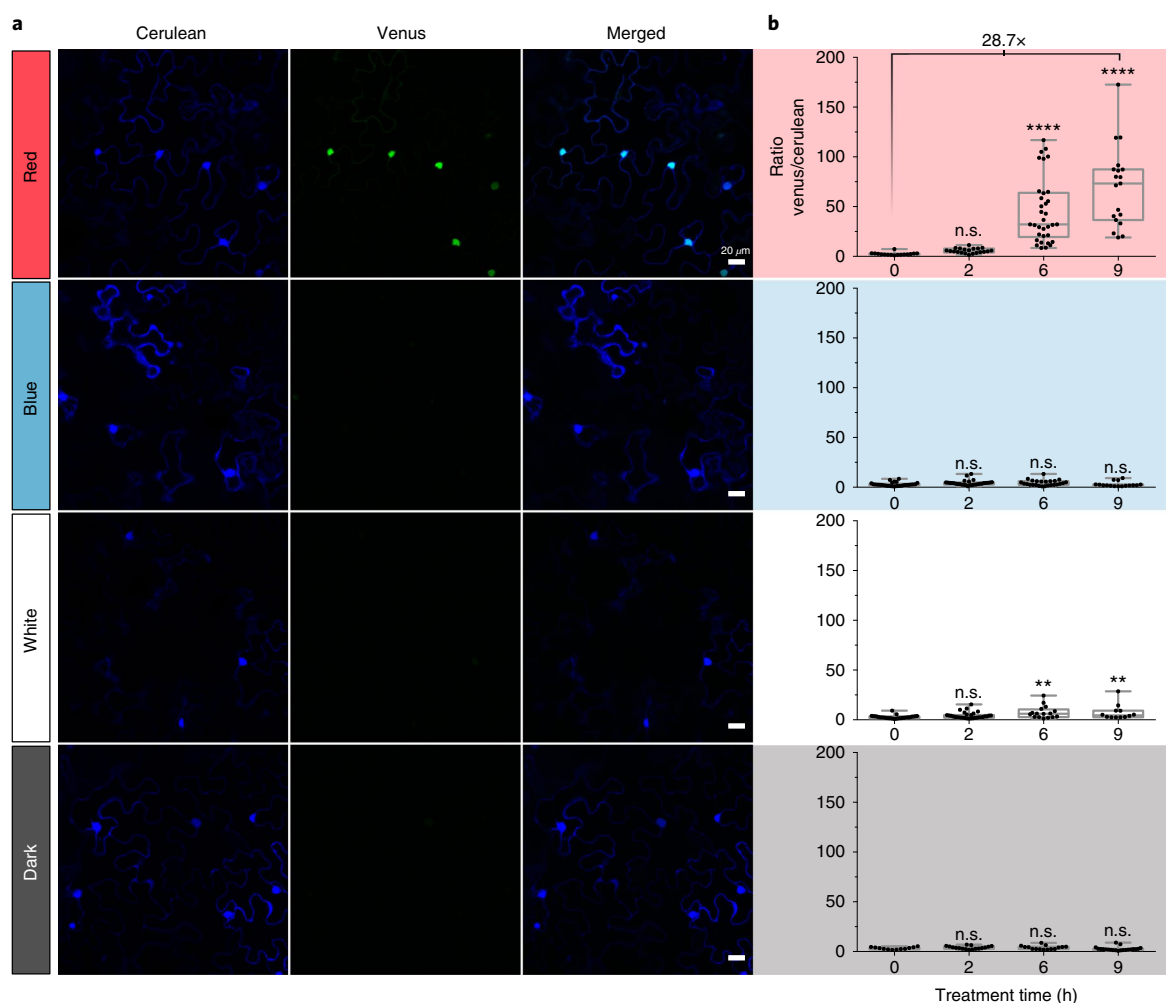
Fig. 5 | Implementation and characterization of PULSE in *N. benthamiana* leaves. a,b, Plants infiltrated with *Agrobacterium* transformed with the plasmids containing PULSE, P_{Opto}–Venus and a constitutively expressed Cerulean cassette were kept in the dark for 2.5 d prior to light treatment for 2 h, 6 h and 9 h (10 µmol m^{-2} s^{-1} red light, 10 µmol m^{-2} s^{-1} blue light, white light or darkness). **a**, Representative fluorescence confocal microscopy images showing Venus and Cerulean fluorescence of samples taken after 9 h. The experiment was performed three times with similar results. **b**, Quantification of nuclear Venus and Cerulean fluorescence-intensity ratios of samples taken at the indicated time points and light conditions. Data are presented in a box plot, with the median (center line), interquartile range (box) and the minimum to maximum values (whiskers); $12 \leq n \leq 34$ nuclei. The statistical significance was determined by a one way-analysis of variance and Dunnett's multiple-comparison test. *P* values are 0.9696, 0.0001 and 0.0001, for 2, 6 and 9 h, respectively, for red-light treatment; 0.3828, 0.0020 and 0.0071, for 2, 6 and 9 h, respectively, for white-light treatment; 0.0643, 0.0727 and 0.9989, for 2, 6 and 9 h, respectively, for blue-light treatment; 0.5051, 0.5251 and 0.7580, for 2, 6 and 9 h, respectively, for dark treatment (***P* < 0.01, ****P* < 0.001, *****P* ≤ 0.0001; n.s., not significant).

of LFY protein (Fig. 4d). We transformed the PULSE plasmids in *Arabidopsis* protoplasts either with or without the optogenetically inducible LFY, and a P_{AtAP1}–FLuc target plasmid. RLuc values indicate that there was expression of LFY–VP16 upon red-light treatment, whereas only basal levels were obtained upon blue-light illumination or in darkness (17.5- and 26.6-fold induction, respectively). The red-light-induced expression of LFY–VP16 led to activation of P_{AtAP1} and achieved FLuc expression induction rates that were 31.4- and 7.4-fold over FLuc expression in blue light and in darkness, respectively (Fig. 4f and Supplementary Fig. 3c).

In planta optogenetic control of gene expression with PULSE. We next evaluated the functionality of PULSE in plants. We constructed a set of vectors for transformation via *Agrobacterium tumefaciens* with all necessary components in binary plasmids. The vectors comprise a reporter gene under the control of PULSE (P_{Opto}), PULSE expressed under a constitutive promoter (either $P_{CaMV35S}$ or $P_{AtUbi10}$) and, optionally, a constitutively expressed reporter

gene as a normalization element and a plant selection cassette (Supplementary Table 1).

We transiently transformed *N. benthamiana* leaves with a construct containing PULSE, a fluorescent protein gene as a reporter (Venus fused to histone H2B for nuclear localization, P_{Opto}–Venus–H2B) and constitutively expressed Cerulean fused to a nuclear localization sequence (NLS) as a normalization element. The plants showed an increase in nuclear Venus/Cerulean fluorescence ratio over time when treated with red light, reaching 28.7-fold induction after 9 h and keeping background levels in blue, dark and white light, demonstrating activation of the system in planta (Fig. 5 and Supplementary Fig. 4). Additionally, we used PULSE to control a β-glucuronidase gene (P_{opto}–GUS) (Supplementary Fig. 5).

In planta optogenetic induction of immunity and conditional subcellular fluorescent targeting of receptors. In plants, signal integration of extracellular stimuli is predominantly mediated by
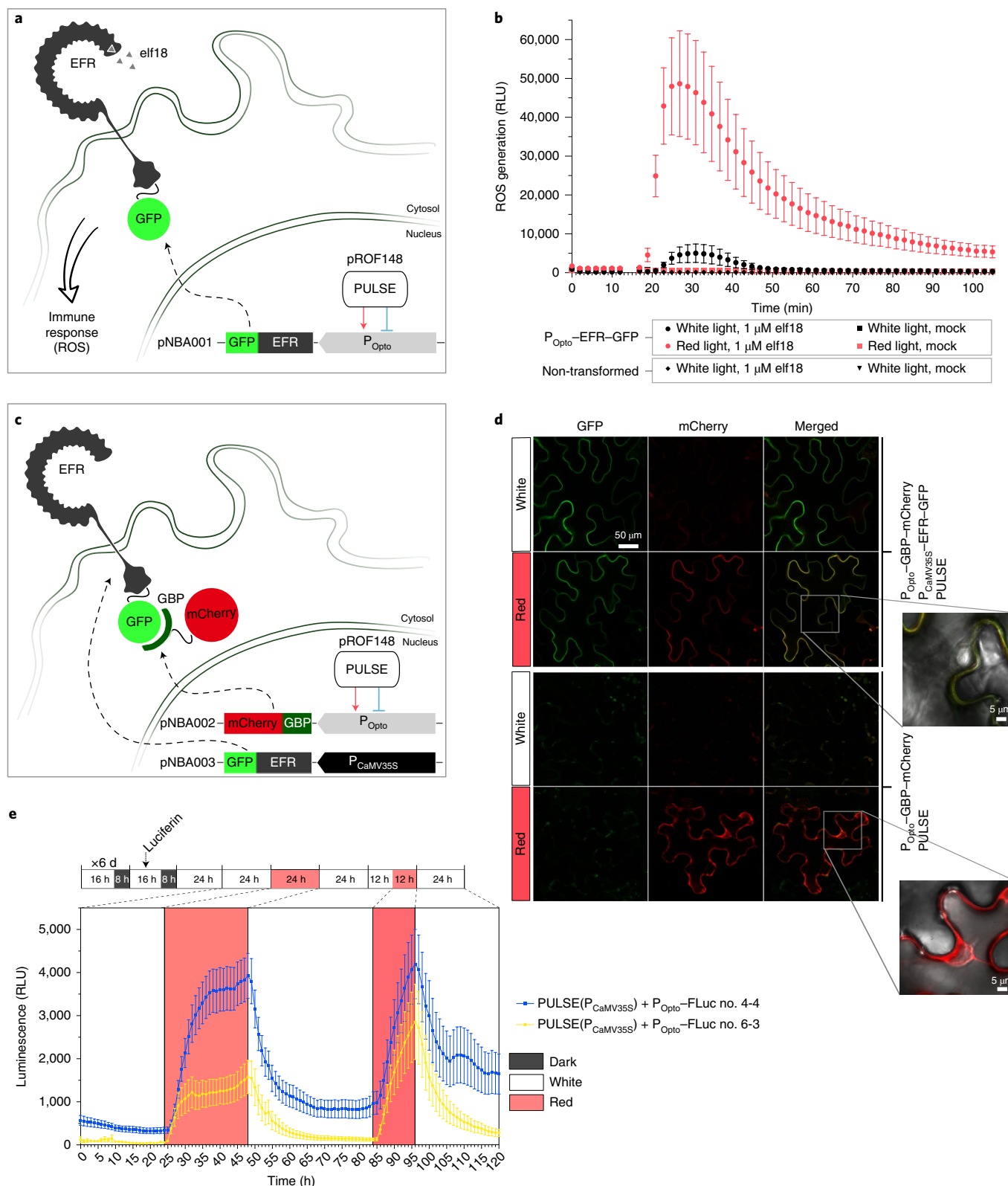
Fig. 6 | In planta optogenetic heterologous induction of immunity and conditional subcellular targeting of receptors, and PULSE functionality in *Arabidopsis* **transgenic lines. a,b,** PULSE-controlled conditional gain of immunity in planta. ROS quantification over time of *N. benthamiana* leaves transformed with PULSE and P_{Opto}–EFR–GFP. Plants transiently transformed were induced with $10\,\mu mol\,m^{-2}\,s^{-1}$ red light for 16 h (control, white light). Disks were collected and treated with $1\,\mu M$ elf18 or mock as indicated. Luminescence mean values and s.e.m. are plotted ($n = 8$ leaf disks from 2 plants). **c,d,** Conditional targeting of receptors by optogenetically controlled expression of a nanobody (GBP–mCherry). Confocal microscopy images of *N. benthamiana* leaves transformed with PULSE, P_{Opto}–GBP–mCherry and $P_{CaMV35S}$–EFR–GFP constructs (control was without $P_{CaMV35S}$–EFR–GFP) that are illuminated as in **b**. **e,** PULSE functionality in *Arabidopsis* plants. Two independent *Arabidopsis* homozygous T3 lines (no. 4-4, no. 6-3) transformed with PULSE controlling P_{Opto}–FLuc ($n = 26$ seedlings, each line) were grown for 8 d and subsequently illuminated as indicated, and their luminescence was determined over time. ×6 d, repeated 6 times, equivalent to 6 d. Mean (background values from wild-type seedlings subtracted, $n = 6$) and s.e.m. are plotted.

membrane-resident receptor and transport complexes. To mechanistically understand their function, we require non-invasive inducible systems that allow transcriptional induction or complex formation with high temporal precision in order to reconstitute these functional entities in homologous as well as heterologous systems. We therefore asked whether PULSE allows the generation of immune-competent leaf epidermal cells by introducing a heterologous-pattern-recognition receptor.

In *Arabidopsis*, recognition of the bacterial peptide microbe-associated molecular pattern (MAMP) elf18 by the plant innate immune EF-Tu receptor (*A. thaliana* (*At*)EFR) results in a fast and transient increase in cellular reactive oxygen species (ROS)[22]. By contrast, *Solanaceae* species, such as *N. benthamiana*, are devoid of EFR and therefore are unable to perceive the elf18 peptide[23]. However, transformation of *N. bethamiana* and *S. lycopersicum* with *At*EFR allows these plants to recognize elf18 and confers increased resistance against phytopathogens, such as *Ralstonia solanacearum*[22,24]. To achieve optogenetically controlled induction of immunity in plants, we expressed an EFR–green fluorescent protein (GFP) fusion protein under the control of PULSE (P_{Opto}–EFR–GFP) in *N. benthamiana* leaf epidermal cells (Fig. 6a). Red-light treatment of leaves for 16 h resulted in a GFP signal at the cell periphery, indicating that EFR–GFP localized to the plasma membrane (Supplementary Fig. 6). To test whether optogenetically controlled EFR provides susceptibility of these cells towards elf18, we applied 1 µM of the elf18 ligand. Indeed, we observed a strong and transient production of ROS roughly 10 min after elf18 application in leaves that had been treated with red light (Fig. 6b). Plants grown in white light exhibited an approximately tenfold lower ROS burst (Fig. 6b), demonstrating light repression by PULSE under ambient light conditions. We did not detect any responses in untransformed tissue and leaves expressing EFR but incubated in the absence of elf18. It should be noted that MAMP-triggered ROS production also relies on a self-amplifying mechanism. ROS spread to neighboring cells where they induce calcium fluxes, which leads to the activation of the ROS-producing protein respiratory burst oxidase homolog protein D (RBOHD)[25,26]. Thus, ROS will be detected even at low background levels of EFR in this system. In conclusion, PULSE can be used for inducing physiological responses in planta in a time-controlled manner.

Next, we tested the applicability of PULSE for conditional targeting of receptors using nanobodies. In mammalian cells, receptor complexes have been reconstituted and modulated using genetically encoded nanobodies[27,28]. Given their small size and their high-affinity binding characteristics, nanobodies can be used to subcellularly relocalize proteins in a stimulus-dependent manner or to visualize endogenous proteins (using fluorophore-tagged nanobodies). We constitutively expressed the immune receptor EFR–GFP in *N. benthamiana* leaf epidermal cells and transformed a genetically encoded anti-GFP nanobody (GFP-binding protein (GBP))[29]. To monitor localization, we additionally fused GBP to mCherry and placed it under the control of PULSE (P_{Opto}–GBP–mCherry) (Fig. 6c). Red-light induction of GBP–mCherry expression in EFR-deficient cells resulted in a cytosolic localization of the soluble protein. By contrast, red-light induction in cells constitutively expressing EFR–GFP resulted in an almost exclusive targeting of the fluorescently tagged nanobody to the plasma membrane (Fig. 6d). This experiment illustrates potential applications using PULSE-driven genetically encoded specific nanobodies for conducting time-resolved conditional targeting of plasma-membrane-localized proteins, such as for targeting proteins for degradation or inhibition similarly to what has been described in animal cells[27,28,30]. This approach could thus provide opportunities to non-invasively control signaling processes in plants.

PULSE functionality in stable *Arabidopsis* transgenic lines. To test the functionality of PULSE in whole plants, we generated transgenic *Arabidopsis* lines using the plasmid coding for PULSE under the control of the $P_{CaMV35S}$ promoter, and P_{Opto}–FLuc as a reporter. We grew seedlings of homozygous T3 plants in a multi-well plate for 7 d, before incubation with luciferin. We quantified luminescence while the plate was subjected to different light treatments (Fig. 6e). Two independent PULSE lines, no. 4-4 and no. 6-3, illustrate that the system is functional with activation levels ranging from 10- to 21-fold, respectively (determined after 12 h of red light, t_{36h}, compared with right before the induction, t_{24h}, with t measured from the start of luminescence determination). Transfer from white light to red light led to activation of expression, and subsequent inactivation was achieved when we moved the plants back to white light (Fig. 6e), demonstrating reversibility of the system, which we also verified in a second cycle. In conclusion, PULSE can control gene expression in whole plants, opening up opportunities for plant research and biotechnology.

Discussion

To study cellular processes, it is helpful to be able to achieve precise spatiotemporal and quantitative control over their regulation. Genetically encoded chemically inducible systems have been widely employed for the targeted manipulation of gene expression and other signaling events in prokaryotic and diverse eukaryotic organisms, including plants[31–33]. However, they suffer from intrinsic drawbacks, including limited temporal and spatial resolution, diffusion effects and constraints to deactivating the system after the application of the inducer, in addition to potential pleiotropic activity and toxicity. Some of these experimental constraints can be solved by using light as an inducer. A plant's requirement for light to grow, however, limits the implementation of optogenetic approaches, as ambient light leads to undesired activation of most currently available light-controlled systems. Consequently, most of the advantages of optogenetics have not yet been applicable in plants.

A recent optogenetic approach using a synthetic, blue-light-gated K⁺ channel (BLINK1)[34] challenged a plant-intrinsic physiological conundrum: how to conserve water under hydric stress by minimizing transpiration without limiting CO_2 uptake, two processes directly regulated by stomatal aperture[35]. Guard-cell-specific expression of BLINK1 in *Arabidopsis* led to accelerated kinetics of ion fluxes (full activation after 2 min of blue-light exposure), with reduction of mean stomatal opening and closure half-life times by 40–70% in comparison with that in wild-type controls. Faster stomatal movements improved gas-exchange efficiency under fluctuating light conditions, resulting in a more efficient use of water without a trade-off in carbon assimilation. This tool profits from the fact that it is applied to a process that is dependent on photosynthesis and therefore already occurs naturally under ambient light.

Towards a more generalized application of optogenetic in plants, we designed an optogenetic tool for the control of gene expression in plants that overcomes their intrinsic challenges—namely, being non-responsive to ambient illumination conditions and only being activated by illumination with a specific, narrow wavelength spectrum. PULSE could in the future be combined with tissue-specific promoters for organs or developmentally specific expression and activity, as is currently done for genetically encoded biosensors and other tools. When using different promoters, the dynamic range of induction might be affected, therefore usage-specific optimizations might be necessary.

By using only the N terminus of PhyB (amino acids 1–650) and the first 100 amino acids of PIF6, we intend to minimize potential interactions of the system with endogenous plant components (EL222 is of bacterial origin, therefore we do not expect any considerable effect on plant signaling). However, we cannot rule out a possible PULSE cross-talk with the endogenous PhyB signaling pathway. This is an unavoidable price to pay in exchange for the added functionality, as this is also the case when using chemically

inducible switches[31,32] or genetically encoded biosensors; for example, some hormone sensors can lead to phenotypes of hormone hypersensitivity[36].

Our strategy can be expanded to develop other optogenetic tools that are compatible with a plant's growth needs. These need not be restricted to transcriptional regulation. They could be extended to the application of selected mammalian optogenetic systems, for example to control cellular receptors, kinase activity and ion and metabolite transporters, among other cellular processes[1,37]. For example, signaling proteins could be engineered for red-light-regulated recruitment to subcellular locations where they activate a signaling cascade, for example to the plasma membrane[38,39]. To prevent activation under white light, the same signaling protein could additionally be targeted for degradation under blue light by being fused to a blue-light-inducible degron[14,40,41]. Alternatively, the signaling protein could be sequestered to the nucleus under white light by being fused to the blue-light-responsive LINuS[42] or LANS[43] systems. Hence, only under exclusive red-light treatment would the protein be targeted to the site of activity in the cytoplasm or plasma membrane and exert its function. We think that, in the future, PULSE will facilitate the targeted manipulation and study of biological processes in plants, including development, growth, hormone signaling and stress responses.

Online content

Any methods, additional references, Nature Research reporting summaries, source data, extended data, supplementary information, acknowledgements, peer review information; details of author contributions and competing interests; and statements of data and code availability are available at https://doi.org/10.1038/s41592-020-0868-y.

References

1. Deisseroth, K. & Hegemann, P. The form and function of channelrhodopsin. *Science* **357**, eaan5544 (2017).
2. Alberio, L. et al. A light-gated potassium channel for sustained neuronal inhibition. *Nat. Methods* **15**, 969–976 (2018).
3. Ye, H., Baba, M. D.-E., Peng, R.-W. & Fussenegger, M. A synthetic optogenetic transcription device enhances blood-glucose homeostasis in mice. *Science* **332**, 1565 (2011).
4. Strickland, D. et al. TULIPs: tunable, light-controlled interacting protein tags for cell biology. *Nat. Methods* **9**, 379–384 (2012).
5. Shin, Y. et al. Spatiotemporal control of intracellular phase transitions using light-activated optoDroplets. *Cell* **168**, 159–171.e14 (2017).
6. van Bergeijk, P., Adrian, M., Hoogenraad, C. C. & Kapitein, L. C. Optogenetic control of organelle transport and positioning. *Nature* **518**, 111–114 (2015).
7. Kolar, K., Knobloch, C., Stork, H., Žnidarič, M. & Weber, W. OptoBase: a web platform for molecular optogenetics. *ACS Synth. Biol.* **7**, 1825–1828 (2018).
8. Müller, K. et al. A red light-controlled synthetic gene expression switch for plant systems. *Mol. Biosyst.* **10**, 1679–1688 (2014).
9. Chatelle, C. et al. A green-light-responsive system for the control of transgene expression in mammalian and plant cells. *ACS Synth. Biol.* **7**, 1349–1358 (2018).
10. Ochoa-Fernandez, R. et al. in *Optogenetics: Methods and Protocols* (ed. Kianianmomeni, A.) 125–139 (Humana Press, 2016).
11. Nash, A. I. et al. Structural basis of photosensitivity in a bacterial light-oxygen-voltage/helix-turn-helix (LOV-HTH) DNA-binding protein. *Comput. Biol.* **108**, 9449–9945 (2011).
12. Motta-Mena, L. B. et al. An optogenetic gene expression system with rapid activation and deactivation kinetics. *Nat. Chem. Biol.* **10**, 196–202 (2014).
13. Moosmann, P., Georgiev, O., Thiesen, H., Hagmann, M. & Schaffner, W. Silencing of RNA polymerases II and III-dependent transcription by the KRAB protein domain of KOX1, a Krüppel-type zinc finger factor. *Biol. Chem.* **378**, 669–677 (1997).
14. Baaske, J. et al. Dual-controlled optogenetic system for the rapid down-regulation of protein levels in mammalian cells. *Sci. Rep.* **8**, 15024 (2018).
15. Ikeda, M. & Ohme-Takagi, M. A novel group of transcriptional repressors in *Arabidopsis*. *Plant Cell Physiol.* **50**, 970–975 (2009).
16. Kelly, J. M. & Lagarias, J. C. Photochemistry of 124-kilodalton Avena phytochrome under constant illumination in vitro. *Biochemistry* **24**, 6003–6010 (1985).
17. Müller, K. et al. Multi-chromatic control of mammalian gene expression and signaling. *Nucleic Acids Res.* **41**, e124 (2013).
18. Li, Z. et al. A potent Cas9-derived gene activator for plant and mammalian cells. *Nat. Plants* **3**, 930–936 (2017).
19. Selma, S. et al. Strong gene activation in plants with genome-wide specificity using a new orthogonal CRISPR/Cas9-based programmable transcriptional activator. *Plant Biotechnol. J.* **17**, 1703–1705 (2019).
20. Simon, R., Igeño, M. I. & Coupland, G. Activation of floral meristem identity genes in *Arabidopsis*. *Nature* **384**, 59–62 (1996).
21. de Felipe, P. et al. E unum pluribus: multiple proteins from a self-processing polyprotein. *Trends Biotechnol.* **24**, 68–75 (2006).
22. Zipfel, C. et al. Perception of the Bacterial PAMP EF-Tu by the receptor EFR restricts *Agrobacterium*-mediated transformation. *Cell* **125**, 749–760 (2006).
23. Kunze, G. et al. The N terminus of bacterial elongation factor Tu elicits innate immunity in *Arabidopsis* plants. *Plant Cell* **16**, 3496–3507 (2004).
24. Lacombe, S. et al. Interfamily transfer of a plant pattern-recognition receptor confers broad-spectrum bacterial resistance. *Nat. Biotechnol.* **28**, 365 (2010).
25. Suzuki, N. et al. Respiratory burst oxidases: the engines of ROS signaling. *Curr. Opin. Plant Biol.* **14**, 691–699 (2011).
26. Gaupels, F., Durner, J. & Kogel, K.-H. Production, amplification and systemic propagation of redox messengers in plants? The phloem can do it all! *N. Phytol.* **214**, 554–560 (2017).
27. Kirchhofer, A. et al. Modulation of protein properties in living cells using nanobodies. *Nat. Struct. Mol. Biol.* **17**, 133 (2009).
28. Gulati, S. et al. Targeting G protein-coupled receptor signaling at the G protein level with a selective nanobody inhibitor. *Nat. Commun.* **9**, 1996 (2018).
29. Schornack, S. et al. Protein mislocalization in plant cells using a GFP-binding chromobody. *Plant J.* **60**, 744–754 (2009).
30. Yu, D. et al. Optogenetic activation of intracellular antibodies for direct modulation of endogenous proteins. *Nat. Methods* **16**, 1095–1100 (2019).
31. Moore, I., Samalova, M., Kurup, S., For, T. & Analysis, M. Transactivated and chemically inducible gene expression in plants. *Plant J.* **45**, 651–683 (2006).
32. Zuo, J. & Chua, N. H. Chemical-inducible systems for regulated expression of plant genes. *Curr. Opin. Biotechnol.* **11**, 146–151 (2000).
33. Andres, J., Blomeier, T. & Zurbriggen, M. D. Synthetic switches and regulatory circuits in plants. *Plant Physiol.* **179**, 862–884 (2019).
34. Cosentino, C. et al. Engineering of a light-gated potassium channel. *Science* **348**, 707–710 (2015).
35. Papanatsiou, M. et al. Optogenetic manipulation of stomatal kinetics improves carbon assimilation, water use, and growth. *Science* **363**, 1456–1459 (2019).
36. Martin-Arevalillo, R. & Vernoux, T. Shining light on plant hormones with genetically encoded biosensors. *Biol. Chem.* **400**, 477–486 (2018).
37. Kolar, K. & Weber, W. Synthetic biological approaches to optogenetically control cell signaling. *Curr. Opin. Biotechnol.* **47**, 112–119 (2017).
38. Levskaya, A., Weiner, O. D., Lim, W. A. & Voigt, C. A. Spatiotemporal control of cell signalling using a light-switchable protein interaction. *Nature* **461**, 997–1001 (2009).
39. Toettcher, J. E., Weiner, O. D. & Lim, W. A. Using optogenetics to interrogate the dynamic control of signal transmission by the Ras/Erk module. *Cell* **155**, 1422–1434 (2013).
40. Renicke, C., Schuster, D., Usherenko, S., Essen, L. O. & Taxis, C. A LOV2 domain-based optogenetic tool to control protein degradation and cellular function. *Chem. Biol.* **20**, 619–626 (2013).
41. Bonger, K. M., Rakhit, R., Payumo, A. Y., Chen, J. K. & Wandless, T. J. General method for regulating protein stability with light. *ACS Chem. Biol.* **9**, 111–115 (2014).
42. Niopek, D. et al. Engineering light-inducible nuclear localization signals for precise spatiotemporal control of protein dynamics in living cells. *Nat. Commun.* **5**, 4404 (2014).
43. Yumerefendi, H. et al. Control of protein activity and cell fate specification via light-mediated nuclear translocation. *PLoS One* **10**, e0128443 (2015).

Methods

Plasmid construction. A description of the plasmid construction can be found in Supplementary Table 1. DNA fragments were released by restriction from existing plasmids, amplified by PCR using primers synthesized by Sigma Aldrich or Eurofins genomic (listed in Supplementary Table 2) or synthesized by GeneArt, Invitrogen. The PCR reactions were performed using Q5 High-Fidelity DNA Polymerase (New England Biolabs). Gel extractions were performed using NucleoSpin Gel and PCR Clean-up Kit (Macherey-Nagel), or Zymoclean Gel DNA Recovery Kit (Zymo Research). Assemblies were performed using the Gibson[44], AQUA[45], GoldenBraid[46] or Golden Gate[47,48] cloning methods prior to transformation into chemically competent *E. coli* strain 10-beta (NEB) or TOP10 (Invitrogen). The plasmid purifications were performed using Wizard Plus SV Minipreps DNA Purification Systems (Promega), NucleoBond Xtra Midi kit (Macherey-Nagel) or GeneJET Plasmid Miniprep Kit (Thermo Scientific). All preparations were tested by restriction enzyme digests and sequencing (GATC-biotech/SeqLab). All restriction enzymes were purchased from New England Biolabs or Thermo Scientific.

***Arabidopsis* protoplast isolation and transformation.** Protoplasts were isolated from 2- to 3-week-old *A. thaliana* plantlet leaves, grown on 12-cm square plates containing SCA medium (0.32 % (wt/vol) Gamborg's B5 basal salt powder with vitamins (bioWORLD), 4 mM $MgSO_4{\cdot}7H_2O$, 43.8 mM sucrose and 0.8% (wt/vol) phytoagar in H_2O, pH 5.8, autoclaved, 0.1% (vol/vol) Gamborg's B5 Vitamin Mix (bioWORLD)) in a 23 °C, 16-h light–8-h dark regime. A floatation method was employed for isolation, and the plasmids were transferred by polyethylene-glycol-mediated transformation as has been described[10]. Briefly, plant leaf material was sliced with a scalpel and incubated in darkness at 23 °C overnight in MMC solution (10 mM MES, 40 mM $CaCl_2{\cdot}H_2O$, 467 mM mannitol, pH 5.8, sterile filtered) containing 0.5% cellulase Onozuka R10 and macerozyme R10 (SERVA Electrophoresis). After release of the protoplasts with a pipette, the suspension was transferred to a MSC solution (10 mM MES, 0.4 M sucrose, 20 mM $MgCl_2{\cdot}6H_2O$, 467 mM mannitol, pH 5.8, sterile filtered) and overlaid with MMM solution (15 mM $MgCl_2$, 5 mM MES, 467 mM mannitol, pH 5.8, sterile filtered). The protoplasts were collected at the interphase and transferred to a W5 solution (2 mM MES, 154 mM NaCl, 125 mM $CaCl_2{\cdot}2H_2O$, 5 mM KCl, 5 mM glucose, pH 5.8, sterile filtered) prior to counting in a Rosenthal chamber. Mixtures of the different plasmids, as described in the figures, to a final amount of 30–35 μg DNA were used to transform 500,000 protoplasts by dropwise addition of a PEG solution (4 g PEG_{4000}, 2.5 ml of 800 mM mannitol, 1 ml of 1 M $CaCl_2$ and 3 ml H_2O). After 8-min incubation, 120 μl MMM and 1,240 μl PCA (0.32% (wt/vol) Gamborg's B5 basal salt powder with vitamins (bioWorld), 2 mM $MgSO_4{\cdot}7H_2O$, 3.4 mM $CaCl_2{\cdot}2H_2O$, 5 mM MES, 0.342 mM L-glutamine, 58.4 mM sucrose, 444 mM glucose, 8.4 μM calcium pantothenate, 2% (vol/vol) biotin from a biotin solution 0.02% (wt/vol) 0.1% (vol/vol) in H_2O, pH 5.8, sterile filtered, 0.1% (vol/vol) Gamborg's B5 Vitamin Mix, 64.52 μg μl⁻¹ ampicillin) were added to get a final volume of 1.6 ml protoplast suspension.

After transformation, protoplasts were divided in 24-well plates in 960-μl aliquots (300,000 protoplasts, necessary to measure 6 technical replicates for both FLuc and RLuc) or in 640-μl aliquots (200,000 protoplasts, necessary to measure 4 technical replicates for both FLuc and RLuc). Afterwards, the plates were either illuminated with light-emitting diode (LED) arrays with the appropriate wavelength and intensity (as indicated in the figures) for 18–20 h at 19–23 °C unless indicated otherwise.

Illumination conditions. Custom-made LED light boxes were used as previously described[10,49]. The panels contain LEDs from Roithner: blue (461 nm), red (655 nm), far-red (740 nm) and white (4,000 K). For treatment with blue, red or far-red light, the intensity was adjusted to 10 μmol m⁻² s⁻¹ unless indicated otherwise. Calculation and conversion of light intensities at given wavelengths can be performed with the online tool www.optobase.rg/converter/. White LEDs were supplemented with blue and far-red LEDs in order to have an equivalent ratio of blue, red and far-red light similar to the sunlight spectra (termed simulated white light here). The intensity of the white light LED was adjusted to 10 μmol m⁻² s⁻¹ for the following wavelength ranges: blue 420–490 nm, red 620–680 nm, and far-red 700–750 nm[50] (see spectra shown in Supplementary Fig. 7). For the *N. benthamiana* GUS experiment, the plants were kept, prior to light treatment, in the plant incubator with fluorescent tubes (cool daylight, OSRAM). Cell and plant handling and sampling was done, when needed, under green LED (510 nm) light, which does not affect the PULSE system. Spectra and intensities were obtained with a spectroradiometer (AvaSpec-ULS2048 with fiber-optic FC-UVIR200-2, AVANTES).

Luciferase protoplasts assay. FLuc and RLuc activities were quantified in intact protoplasts as detailed elsewhere[10]. Six technical replicates of 80-μl protoplast suspensions (approximately 25,000 protoplasts) were pipetted into two separate 96-well white flat-bottom plates (Costar) for simultaneous parallel quantification of both luciferases. Addition of 20 μl of either FLuc substrate (0.47 mM D-luciferin (Biosynth AG), 20 mM tricine, 2.67 mM $MgSO_4{\cdot}7H_2O$, 0.1 mM EDTA·$2H_2O$, 33.3 mM dithiothreitol, 0.52 mM adenosine 5′-triphosphate, 0.27 mM acetyl–coenzyme A, 5 mM NaOH, 264 μM $MgCO_3{\cdot}5H_2O$, in H_2O, pH 8) or RLuc substrate (0.472 mM coelenterazine stock solution in methanol, diluted directly before use,

1:15 in PBS) was performed prior luminescence determination in a plate reader (determination of 20-min kinetics, integration time 0.1 s). RLuc luminescence was measured with a BertholdTriStar2 S LB 942 multimode plate reader, and FLuc luminescence was measured with a Berthold Centro XS3 LB 960 microplate luminometer. When applicable, the FLuc/RLuc ratio was determined, and the average of the replicates was plotted with the s.e.m. ($n = 4$–6).

RNA isolation and quantitative reverse-transcription PCR. Protoplasts were isolated and transformed as has been described. The protoplasts were kept in the dark, at room temperature, for 16 h prior illumination treatment. At the indicated time points (15 min, 30 min, 1 h, 2 h, 4 h, 4 h 15 min, 4 h 30 min, 6 h, 7 h) and illumination conditions (4 h red light, followed by 3 h blue light), samples containing approximately 1×10^6 protoplasts were collected by centrifugation (10 min, 100g) and were frozen in liquid N_2 for RNA extraction. The RNA was extracted with a PeqGold Plant RNA kit following the manufacturer specifications. The samples were treated with DNase I (Thermo Scientific). The complementary DNA was synthesized from 500 ng of the RNA samples, using the Revert Aid Reverse Transcriptase (Thermo Scientific) and diluted to 1:100 prior to quantitative PCR. Expression levels on the samples were measured in duplicates using SYBR Green Master Mix (Bio-Rad) with specific primer pairs in a real-time PCR cycler CFX96 (Bio-Rad) as has been described[51]. A DNA mass standard for each gene was prepared in serial dilutions of 1×10^2–1×10^7 copies and measured in parallel with the samples. The genes *TIP41*-like family protein, *TIP41L* (*At4g34270*), and elongation factor, *EF* (*At5g19510*), were used as an internal reference genes. Starting quantity values of the samples were calculated using the mass standard curve and normalized with the internal reference gene. Primer pairs used to amplify the DNA mass standard were oROF422/oROF423 for FLuc, oROF518/oROF519 for TIP41L and EF STD 5′/3′[51] for EF. Specific primer pairs used for the quantitative PCR were oROF424/oROF425 for FLuc cDNA, oROF514/oROF515 for TIP41L cDNA and EFc RT 5′/3′[51] for EF cDNA (Supplementary Table 2).

***A. tumefaciens* transformation.** Electro-competent *A. tumefaciens* strains C58 (pM90), GV3101 (pM90), containing pSOUP helper plasmid, or AGL1 were transformed with the plasmid of interest. Clones growing in YEP medium (10 g l⁻¹ yeast extract, 10 g l⁻¹ Bacto Peptone, 86 mM NaCl, pH 7.0) supplemented with appropriate antibiotics were selected, and each transcriptional unit was confirmed by colony PCR using Q5 DNA polymerase (New England Biolabs).

Transient transformation of *N. benthamiana* plants. *A. tumefaciens* cultures were adjusted to optical density measured at a wavelength of 600 nm (OD_{600}) = 0.1–0.2 in infiltration medium (10 mM $MgCl_2$, 10 mM MES, 200 μM acetosyringone, in H_2O, pH 5.6). The cultures were mixed in a volume ratio of 1:1 with an *A. tumefaciens* culture tranformed with a plasmid encoding the RNA-silencing suppressor p19. The cultures were incubated for 3 h at room temperature in the dark prior to infiltration through the adaxial part of leaves of 4- to 5-week-old *N. benthamiana* that were grown in a greenhouse as has been described[52]. The plants were incubated for 2–3 d in the indicated illumination conditions prior to light treatment and analysis by microscopy or enzymatic GUS reporter assay.

GUS reporter assay in *N. benthamiana* leaves. After the illumination of the plants transformed with the construct BM00369 as depicted in the Supplementary Fig. 5, 2 disks, with a diameter of 0.8 cm, from different leaves for each illumination treatment were cut and incubated on GUS substrate (100 mM Na_2HPO_4, 100 mM NaH_2PO_4, adjusted to pH 7.0, 2 mM $K_3Fe(CN)_6$, 2 mM $K_4Fe(CN)_6$, 2 mM X-Gluc, 0.20% Triton X-100, in H_2O) for 3 h at 37 °C in the dark[53]. The stained disks were washed several times with 70% ethanol to remove the chlorophylls, and the pictures were taken with a Nikon D3200 camera.

Confocal imaging of *N. benthamiana* leaf material. For the experiments of optogenetically controlled Venus, leaves of 1 or 2 plants for each condition were transiently transformed with *Agrobacterium* containing the pROF346 construct and incubated for 2.5 d in the dark, and afterwards illuminated for 2 h, 6 h or 9 h with the appropriate wavelength as indicated in Fig. 5a,b. Samples were taken at the indicated time points from three different areas of the leaves of the two plants and were imaged with a LSM 780 Zeiss laser scanning confocal microscope. The constitutive Cerulean was excited with a diode 405 nm. The optogenetically controlled Venus expression was excited with an Argon laser at 514 nm. The emission was detected at 440–500 nm for Cerulean and 516–560 nm for Venus. For each condition, at least six images with two to eight nuclei per image were generated. The fluorescence intensities of nuclei were quantified using ImageJ. For each nucleus, an area was selected by using the elliptical selection tool and the mean gray values of the Cerulean and Venus channels were measured, respectively. The ratio of Venus and Cerulean was calculated and expressed in percentage, and plotted for 12–34 nuclei. In particular, Red: t_{0h} $n = 16$; t_{2h} $n = 21$, t_{6h} $n = 34$, t_{9h} $n = 19$; Blue: t_{0h} $n = 29$, t_{2h} $n = 29$, t_{6h} $n = 25$, t_{9h} $n = 16$, White: t_{0h} $n = 29$, t_{2h} $n = 31$, t_{6h} $n = 16$, t_{9h} $n = 12$, Dark: t_{0h} $n = 12$, t_{2h} $n = 17$, t_{6h} $n = 15$, t_{9h} $n = 21$.

For the experiments of conditional targeting and immunity control, *N. benthamiana* transiently transformed with the constructs pROF148 and pNBA002, either with or without pNBA003, were grown for 2 d in a 16-h simulated white

light–8-h dark cycle (Supplementary Fig. 7); thereafter, half the plants were further incubated in red light for 16 h after the experiments to induce expression, and the other plants were grown in simulated white light for 16 h (control). The control plants were further grown for 16 h after the experiments in red light to induce expression as control for successful transformation. Samples were taken for confocal observation. Confocal laser scanning microscopy was performed with a Leica SP8 confocal microscope using a ×20/0.75 HC PL APO CS IMM CORR lens with a scanning speed of 200 Hz. EFR–GFP and GBP–mCherry were excited with a white-light laser at 488 nm and 561 nm, respectively. The emission was detected at 500–550 nm for GFP and 575–630 nm for mCherry.

ROS burst assay. Samples were collected from *N. benthamiana* leaves transformed with the constructs pROF148 and pNBA001, or only infiltration buffer (two plants were used for each illumination treatment). ROS production was determined using a BMG CLARIOstar plate reader, following the protocol by Trujillo[54] for *Arabidopsis* leaves with the following modifications: samples were prepared with a 4-mm biopsy puncher and placed in 150 μl sterile tap water for 3 h in the dark to get rid of any ROS production originating from the sample collection before elf18 or control treatment. Approximately 20 min before addition of 1 μM elf18, water was removed from leaf samples and replaced with reaction solution[54], and samples were incubated for *about* 3 min before background measurement of ROS production was performed for about 15 min, followed by addition of reaction solution with elf18 or without (mock control).

Stable transformation of *A. thaliana*. *A. thaliana* ecotype Columbia plants aged 4–5 weeks that were grown in a plant chamber (16-h light–8-h dark, 22 °C) were transformed via *A. tumefaciens* by floral dip, as has been described[55] with minor modifications. *Agrobacterium* cells transformed with the BM00654 construct were grown to OD_{600} values between 0.6 and 0.9, centrifuged and gently resuspended in 2.4 g l⁻¹ Murashige and Skoog medium including vitamins (Duchefa Biochemie), 5% (wt/vol) sucrose, 0.05% (vol/vol) Silwet L-77 (bioWORLD) and 222 nM 6-benzylaminopurine (Duchefa Biochemie).

Transformants were selected by seeding in SCA plates (0.32 % (wt/vol) Gamborg's B5 basal salt powder with vitamins (bioWORLD), 4 mM MgSO₄·7H₂O, 43.8 mM sucrose, 0.8 % (wt/vol) phytoagar, 0.1% (vol/vol) Gamborg's B5 Vitamin Mix (bioWORLD), pH 5.8) containing 30 μg ml⁻¹ kanamycin (Duchefa Biochemie) and 150 μg ml⁻¹ ticarcillin disodium/potassium clavulanate (Duchefa Biochemie). The positive T₁ plants were checked for expression of the reporter/normalization gene when possible, and the T2 seeds were collected and selected in kanamycin-containing medium. The lines exhibiting a segregation ratio 3:1 (resistant to sensitive) were propagated until a T₃ generation, and homozygous lines were selected and used for further experiments. The transgenic PULSE lines are functional and viable.

Luciferase assay in *A. thaliana* plants. Seeds from the *A. thaliana* lines ($n = 26$ for the PULSE lines, $n = 6$ for the wild-type controls) were seeded in individual wells of white 96-well white flat-bottom plates (Costar), containing 200 μl of 2.4 g l⁻¹ Murashige and Skoog medium including vitamins (M0222, Duchefa Biochemie) and 0.8 % (wt/vol) phytoagar (bioWORLD). They were kept for 3–4 d at 4 °C in the dark, and were illuminated for 1 h with simulated white light (see spectra in Supplementary Fig. 7) on the fourth day. Then, the plate was placed in simulated white light with photoperiod (16-h light–8-h dark) for 4 d. Addition of 20 μl FLuc substrate 1.667 mM D-luciferin (from a 20 mM stock in DMSO, Biosynth AG) and 0.01% Triton X-100 in H₂O was performed on the fourth day prior starting the measurements. The plate was sealed with an optically clear film (Sarstedt) that was thinly perforated. Luminescence was measured, 1–2 d after addition of the substrate, in a Berthold Centro XS3 LB 960 microplate reader every hour for several days (1-min delay, 0.5 s integration time) while being illuminated as indicated. The background readout levels of wild-type *Arabidopsis* seedlings were averaged, and the value was subtracted from the rest of the lines for each time point.

Sample size, replication and statistics. Data shown in the figures are representative of at least two independent experiments. The sample number per experiment is indicated in each corresponding figure. Plotting and statistical tests were performed with GraphPad or MATLAB software.

Reporting Summary. Further information on research design is available in the Nature Research Reporting Summary linked to this article.

Data availability
Raw and associated data generated with plate-reader-, RT-qPCR- and microscope-specific software that support the findings of this study are available from the corresponding author upon request. The plasmids used in all experiments are available at AddGene, and the plasmid maps at the public repository JBEI-ICE (https://public-registry.jbei.org/folders/577). Source data are provided with this paper.

Code availability
The numerical integration, fitting process and identifiability analysis with the profile likelihood method were performed in MATLAB using the freely available Data2Dynamics software. Details relative to the equations used can be found in the Supplementary Note. Source data are provided with this paper.

References
44. Gibson, D. G. et al. Enzymatic assembly of DNA molecules up to several hundred kilobases. *Nat. Methods* **6**, 343 (2009).
45. Beyer, H. M. et al. AQUA Cloning: a versatile and simple enzyme-free cloning approach. *PLoS One* **10**, e0137652 (2015).
46. Sarrion-Perdigones, A. et al. GoldenBraid 2.0: a comprehensive DNA assembly framework for plant synthetic biology. *Plant Physiol.* **162**, 1618 (2013).
47. Binder, A. et al. A modular plasmid assembly kit for multigene expression, gene silencing and silencing rescue in plants. *PLoS One* **9**, e88218 (2014).
48. Weber, E., Engler, C., Gruetzner, R., Werner, S. & Marillonnet, S. A modular cloning system for standardized assembly of multigene constructs. *PLoS One* **6**, e16765 (2011).
49. Müller, K., Zurbriggen, M. D. & Weber, W. Control of gene expression using a red- and far-red light–responsive bi-stable toggle switch. *Nat. Protoc.* **9**, 622 (2014).
50. Sellaro, R. et al. Cryptochrome as a sensor of the blue/green ratio of natural radiation in *Arabidopsis*. *Plant Physiol.* **154**, 401 (2010).
51. Bauer, P. Regulation of iron acquisition responses in plant roots by a transcription factor: regulation of iron acquisition responses. *Biochem. Mol. Biol. Educ.* **44**, 438–449 (2016).
52. Vazquez-Vilar, M. et al. GB3.0: a platform for plant bio-design that connects functional DNA elements with associated biological data. *Nucleic Acids Res.* **45**, 2196–2209 (2017).
53. Naranjo-Arcos, M. A. et al. Dissection of iron signaling and iron accumulation by overexpression of subgroup Ib bHLH039 protein. *Sci. Rep.* **7**, 10911 (2017).
54. Trujillo, M. in *Environmental Responses in Plants: Methods and Protcools* (ed. Duque, P.) 323–329 (Humana Press, 2016).
55. Clough, S. J. & Bent, A. F. Floral dip: a simplified method for *Agrobacterium*-mediated transformation of *Arabidopsis thaliana*. *Plant J.* **16**, 735–743 (1998).

Author contributions
R.O.F., N.B.A., L.-A.K., J.B.M. and S.M.B. designed and cloned the constructs. S.M.B. performed preliminary tests and R.O.F. conducted all *Arabidopsis* protoplasts experiments. F.-G.W. and R.E. developed the mathematical model. R.O.F., N.B.A., J.S. and L.-A.K. contributed to the establishment of PULSE in planta. N.B.A. conducted the conditional targeting and immunity induction in planta. R.O.F. and G.G. generated the transgenic *Arabidopsis* PULSE lines and performed the experiments. R.O.F., N.B.A., T.O., R.S. and M.D.Z. designed the experiments. J.T., W.W., T.O., R.S. and M.D.Z. supervised the research. T.O., R.S. and M.D.Z. analyzed the data and discussed results. M.D.Z. planned and directed the project. R.O.F. and M.D.Z. designed the system and wrote the initial manuscript with input from all authors. All authors contributed to editing and read the final version of the manuscript.

Competing interests
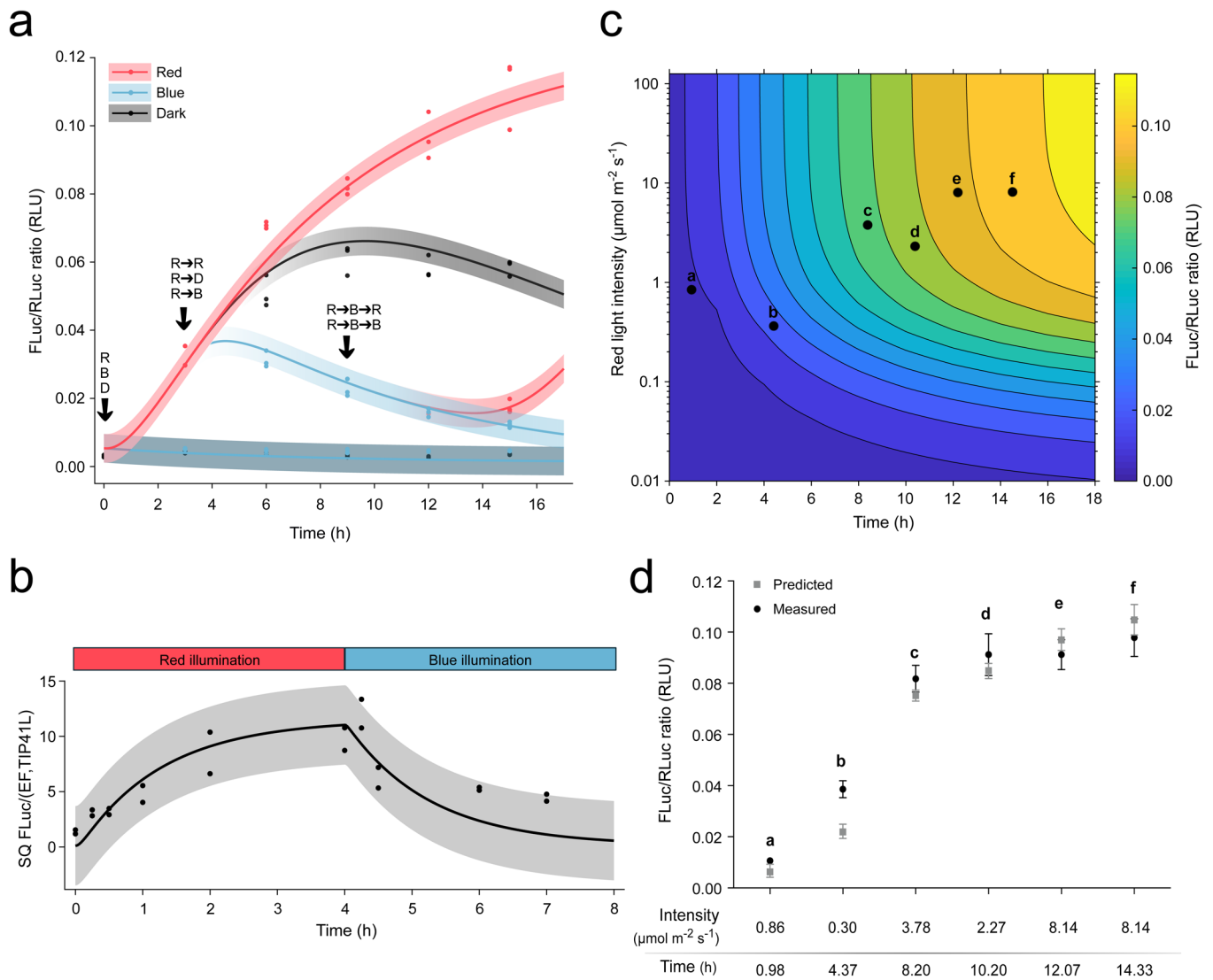The authors declare no competing interests.

Additional information
Extended data is available for this paper at https://doi.org/10.1038/s41592-020-0868-y.

Supplementary information is available for this paper at https://doi.org/10.1038/s41592-020-0868-y.

Correspondence and requests for materials should be addressed to M.D.Z.

Peer review information Nina Vogt was the primary editor on this article and managed its editorial process and peer review in collaboration with the rest of the editorial team.

Reprints and permissions information is available at www.nature.com/reprints.

Extended Data Fig. 1 | Model-based functional characterization, and prediction and validation of PULSE function. a,b, Quantitative characterization of On-Off PULSE kinetics and reversibility. PULSE-driven FLuc expression assays in Arabidopsis protoplasts. (**a**) FLuc/RLuc ratios for protein expression kinetics, $n = 6$ protoplast samples. (**b**) Normalized starting quantity (SQ) of FLuc transcript to the SQ geometric mean of EF and TIP41L transcripts (internal normalization controls), $n = 2$ technical replicates for each transcript (**b**). Protoplasts were transformed and kept in the dark, 12 h for protein (**a**) and 16 h for mRNA (**b**) determination, followed by illumination with either 10 μmol m^{-2} s^{-1} of red or blue light, or kept in darkness. Arrows indicate the time point where the samples were split into different illumination conditions, for example, red to dark, red to blue (On-Off), red to blue to red (On-Off-On). The curves are the fits to the ODE-based model. The shaded areas represent the error bands as calculated in 95% confidence intervals with a constant Gaussian error model using the profile likelihood method. **c**, Model aided prediction of PULSE-controlled protein expression levels as a function of red light intensities and illumination times. The calibrated model yields estimated FLuc/RLuc expression ranges (heatmap). **d**, Experimental validation of the model predictions of the operating range of PULSE. Selected model simulated expression levels at different red light intensities and illumination times as indicated in (**c**) were experimentally tested and the resulting FLuc/RLuc ratios (means and 2xSEM are plotted, $n = 6$ protoplast samples for each condition, black circles) were compared to the predicted values (grey squares). RLU = Relative Luminescence Units.

nature research

Corresponding author(s): Matias D. Zurbriggen

Last updated by author(s): Jun 18, 2020

Reporting Summary

Nature Research wishes to improve the reproducibility of the work that we publish. This form provides structure for consistency and transparency in reporting. For further information on Nature Research policies, see Authors & Referees and the Editorial Policy Checklist.

Statistics

For all statistical analyses, confirm that the following items are present in the figure legend, table legend, main text, or Methods section.

n/a	Confirmed	
☐	☒	The exact sample size (n) for each experimental group/condition, given as a discrete number and unit of measurement
☐	☒	A statement on whether measurements were taken from distinct samples or whether the same sample was measured repeatedly
☐	☒	The statistical test(s) used AND whether they are one- or two-sided *Only common tests should be described solely by name; describe more complex techniques in the Methods section.*
☒	☐	A description of all covariates tested
☐	☒	A description of any assumptions or corrections, such as tests of normality and adjustment for multiple comparisons
☐	☒	A full description of the statistical parameters including central tendency (e.g. means) or other basic estimates (e.g. regression coefficient) AND variation (e.g. standard deviation) or associated estimates of uncertainty (e.g. confidence intervals)
☐	☒	For null hypothesis testing, the test statistic (e.g. F, t, r) with confidence intervals, effect sizes, degrees of freedom and P value noted *Give P values as exact values whenever suitable.*
☒	☐	For Bayesian analysis, information on the choice of priors and Markov chain Monte Carlo settings
☒	☐	For hierarchical and complex designs, identification of the appropriate level for tests and full reporting of outcomes
☒	☐	Estimates of effect sizes (e.g. Cohen's d, Pearson's r), indicating how they were calculated

Our web collection on statistics for biologists contains articles on many of the points above.

Software and code

Policy information about availability of computer code

Data collection

For experiments where luciferase luminescence was measured in plant protoplasts (Fig. 2b,3c,4b,4e,4f; Extended Data Fig. 1a,1d; Supplementary Fig. 1a,1b,1c,3a,3b,3c) and Arabidopsis seedlings (Figure 6e): the software used for acquisition in the plate reader is MikroWin (Berthold).
For experiments of measurement of transcripts (Figure 3d): the software used for acquisition is CFX Manager software (Biorad).
For experiments of Venus/Cerulean microscopy in Nicotiana leaves (Figure 5 and Supplementary Figure 4): the microscope acquisition software is ZEN 2.3 SP1.
For experiments of ROS quantification in Nicotiana leaves (Figure 6b): the plate reader acquisition is MARS Data Analysis Software (BMG Labtech).
For experiments of microscopy acquisition of GFP and mCherry fluorescence in Nicotiana leaves (Figure 6d and Supplementary Figure 6): the microscope acquisition software is Leica Application Suite X (LAS X).

| Data analysis | All data analysis, graph display, and statistics were performed with GraphPad software with the exception of Extended Data Fig. 1a,1b,1c, Supplementary Fig. 2,8,9,10,11 that were performed with MATLAB.
The numerical integration, fitting process and identifiability analysis with the profile likelihood method were performed in MATLAB using the freely available Data2Dynamics software (DOI: 10.1093/bioinformatics/btv405). Details relative to the equations used can be found in the Supplementary Information.
For experiments of measurement of transcripts (Figure 3d): determinations of transcript starting quantity were made with the CFX Manager software (Biorad).
For experiments of Venus/Cerulean microscopy in Nicotiana leaves (Figure 5 and Supplementary Figure 4): the nuclear fluorescent intensity determinations were made with ImageJ.
The analysis of DNA sequences and the construction of plasmid maps were performed with Geneious.
The composition of microscopy Figures was performed with ImageJ and Omero. |
|---|---|

For manuscripts utilizing custom algorithms or software that are central to the research but not yet described in published literature, software must be made available to editors/reviewers. We strongly encourage code deposition in a community repository (e.g. GitHub). See the Nature Research guidelines for submitting code & software for further information.

Data

Policy information about availability of data

All manuscripts must include a data availability statement. This statement should provide the following information, where applicable:

- Accession codes, unique identifiers, or web links for publicly available datasets
- A list of figures that have associated raw data
- A description of any restrictions on data availability

Source data for the figures are available (Source Data .xls files). Raw and associated data generated with plate-reader-, RT-qPCR- and microscope-specific software that support the findings of this study are available from the corresponding author upon request. The plasmids used in all experiments are available at AddGene and the plasmid maps at the public repository JBEI-ICE (https://public-registry.jbei.org).

Field-specific reporting

Please select the one below that is the best fit for your research. If you are not sure, read the appropriate sections before making your selection.

☒ Life sciences ☐ Behavioural & social sciences ☐ Ecological, evolutionary & environmental sciences

For a reference copy of the document with all sections, see nature.com/documents/nr-reporting-summary-flat.pdf

Life sciences study design

All studies must disclose on these points even when the disclosure is negative.

| Sample size | The sample size was chosen according to the state of the art for experimental setups comprising light-inducible switches (optogenetics) in animal and plant cells, these numbers are according to our experience adequate for the kind of experiments and measurements performed:

Experiments where luminescence was measured in plant protoplasts (Fig. 2b,3c,4b,4e,4f; Extended Data Fig. 1a,1d; Supplementary Fig. 1a,1b,1c,3a,3b,3c) three to six distinct protoplast samples were taken for each light condition and/or time point. The FLuc and RLuc activities were measured over 20 min with a repeated measurement set up. The average curve values integrated over time (excluding uptake of substrate and decay of the signal time ranges) were used to further process the data. The ratio FLuc/RLuc was calculated, when applicable, for each one of the distinct protoplast samples and plotted together with the corresponding average and SEM. The n corresponding to the distinct protoplast samples measured for FLuc and RLuc is indicated in the caption of each figure. Extended Data Fig. 1a: n = 3; Fig. 2b,3c,4f; Extended Data Fig. 1d; Supplementary Fig. 1a,1b,1c: n = 6; Fig. 4b,4e; Supplementary Fig. 3a,3b: n = 4.

Transcript/mRNA determinations (Extended Data Fig. 1b): for each illumination/time condition, protoplast samples were taken, RNA extracted and cDNA generated. For each sample, two technical replicates were used for the quantification of each transcript (FLuc, EF, TIP41L). Plotted data are the ratio of FLuc/geometric mean (EF, TIP41L) for both replicates.

Venus/Cerulean fluorescence microscopy determinations in Nicotiana leaves (Figures 5 and Supplementary Figure 4): leaves of two plants were infiltrated for each illumination condition (except for dark treatment, one plant). Samples were taken at indicated time points from three different areas of the two plants for fluorescence confocal microscopy observation. At least 6 images, with 2 to 8 nuclei per image, were taken for each condition. Representative images are shown. The images were used to determine the intensity of Venus and Cerulean for each nucleus. The plots show the nuclear Venus/Cerulean ratio. The number of nuclei analyzed are $12 \leq n \leq 34$. In particular, Red: t0h n = 16; t2h n = 21, t6h n = 34, t9h n = 19; Blue: t0h n = 29, t2h n = 29, t6h n = 25, t9h n = 16, White: t0h n = 29, t2h n = 31, t6h n = 16, t9h n = 12, Dark: t0h n = 12, t2h n = 17, t6h n = 15, t9h n = 21.

For experiments of ROS quantification in Nicotiana leaves (Figure 6b): leaves of two plants were infiltrated for each illumination condition. Four disks from each plant (n = 8 in total) were taken for ROS quantification. Shown data are the average for the eight disks for each condition, and determined over time.

GFP and mCherry fluorescence microscopy determination in Nicotiana leaves (Figure 6d and Supplementary Figure 6): two leaves, each of two different Nicotiana plants for each construct combination and illumination condition were used for microscopy observation. One to two images were taken with a Leica SP8 confocal microscope for each condition. Representative images are shown. |
|---|---|

Luminescence determinations in Arabidopsis seedlings (Figure 6e): seeds from two independent A. thaliana PULSE homozygous T3 lines (#4-4, #6-3) were placed in individual microplate wells with media (n = 26 for each of both PULSE lines, n = 6 for the wild type controls), incubated under different illumination conditions as indicated, and luminescence determined over time in the plate reader. Data shown are the average and SEM for each line (wild type background values were averaged and subtracted).

For experiments where GUS assay in Nicotiana leaves was performed (Supplementary Figure 5): two disks from different infiltrated leaves for each illumination treatment were cut and incubated on GUS substrate.

| Data exclusions | Statistical analysis as described in DOI: 10.1093/nar/gnh157 was used to exclude experimental outliers in the experiment shown in Figure 4e. |

| Replication | All experimental data shown was produced experimentally in at least two independent experiments (different biological material, different batches of plants and/or protoplasts). Data shown are representative, the total amount of experiments performed are: |

Figure 2b: four independent experiments.

Figure 3c: four independent experiments.

Figure 4b and Supplementary Figure 3a: two independent experiments.
Figure 4e and Supplementary Figure 3b: four independent experiments.
Figure 4f and Supplementary Figure 3c: four independent experiments. The constitutive controls were included in two of the experiments.

Figure 5 and Supplementary Figure 4: three independent experiments.

Figure 6b and Supplementary Figure 6: three independent experiments.
Figure 6d: three independent experiments.
Figure 6e: four independent experiments with slightly different illumination schemes.

Extended data Figure 1a: two independent experiments. Albeit one without normalization element.
Extended data Figure 1b: two independent experiments.
Extended data Figure 1d: two independent experiments.

Supplementary Figure 1a: three independent experiments.
Supplementary Figure 1b: two independent experiments, albeit different light intensities were tested.
Supplementary Figure 1c: two independent experiments, albeit different light intensities were tested.

Supplementary Figure 5: two independent experiments.

| Randomization | Not relevant to our study as the operator cannot influence the outcome of the measurement |

| Blinding | In general different conditions, i.e. illumination treatments (and hardware), times, transformation batches, etc. are and must be known by the operator. In any case, the operator cannot influence the outcome of the measurement. |

Reporting for specific materials, systems and methods

We require information from authors about some types of materials, experimental systems and methods used in many studies. Here, indicate whether each material, system or method listed is relevant to your study. If you are not sure if a list item applies to your research, read the appropriate section before selecting a response.

Materials & experimental systems

n/a	Involved in the study
☒	☐ Antibodies
☒	☐ Eukaryotic cell lines
☒	☐ Palaeontology
☒	☐ Animals and other organisms
☒	☐ Human research participants
☒	☐ Clinical data

Methods

n/a	Involved in the study
☒	☐ ChIP-seq
☒	☐ Flow cytometry
☒	☐ MRI-based neuroimaging